CIMAC CONGRESS 25
ZURICH, MAY 19 – 23, 2025

2025 | 466

1st methanol generation of valve spindles and seat ring for newbuildings and retrofit

Mechanics, Materials & Coatings

Janis Kimm, Märkisches Werk GmbH

Oliver Lehmann, Märkisches Werk GmbH
Victoria Jakob, Märkisches Werk GmbH

ABSTRACT

In the pursuit towards net-zero CO2 emissions, methanol is currently one of the most promising alternative fuels in the large bore engine industry, alongside hydrogen and ammonia. The stepwise introduction of methanol up to 100 % by blending it with diesel leads to an increasing material challenge due to its chemical properties. Methanol as a substance from the group of alcohols is often used as a cleaning agent. As a result, the exposure to methanol raises the question about material compatibility regarding existing valve materials. In case of lifetime, material degradation is to be expected due to corrosive attack. While the material compatibilities of valve train components for existing large-bore diesel and natural gas engines is well understood, this is not yet the case for large-bore methanol engines.

This paper deals with the retrofit approach for methanol for intake and exhaust valve spindle/valve seat ring pairings from field component investigation to material screening. Typical intake and exhaust pairings for diesel applications running with 10% diesel and 90% methanol were investigated to understand the material compatibility. Indications of tribo-corrosive attack and methanol-specific material damage on both valves and seat rings were observed due to methanol and its combustion by-products methanoic acid. The cast steel seat ring was found to exhibit attack along the grain boundaries, even in areas without direct contact to the valve. The Stellite 12 hardfaced seating surface on the exhaust valve shows untypical outbreaks from the surface. The appearances founded are clearly defined locally. From this it can be concluded that the material damage observed is less due to plastic deformation than to tribo-corrosive attack.

Considering the field findings, as a next step the effect of methanol and its combustion by-product methanoic acid on material degradation of existing valve materials were screened. A specially developed test setup was designed and manufactured. Series of tests, each with 100,000 load cycles, were carried out in methanol and methanoic acid at 100°C and at 400°C, respectively. To simulate the valve and seat ring pairing correctly, special samples from typical valve materials were manufactured and tested with application-typical surface pressures. The results show higher wear in methanol at 100°C compared with 400°C, especially for the materials 1.4882 (LV21-43), 2.4952 (Nimonic 80a) and 1.4718 (X45CrSi9-3). At an elevated temperature of 400°C in both methanol and methanoic acid atmosphere, the results for all materials except Stellite 12 point out less wear. In a comparison of all measured results, the MW WR Superalloy MW-H5428-8 shows the lowest wear values in each case. Valves in large engines experiences 108 load cycles. Therefore, a further development of the MW WR Superalloys can be certainly be expected midterm with increasing operating hours in methanol.

Based on experience from methanol field tests, extensive material screening tests and almost 80 years of experience in valve production, Märkische Werk GmbH presents its first generation of methanol valve spindles and seat rings for intake and exhaust.

1 INTRODUCTION

In the pursuit of net zero CO_2 emissions, methanol is currently one of the most promising alternative fuels in the large engine industry alongside hydrogen and ammonia. From 1974 to 2021 the worldwide CO_2 concentration has increased by about 24 % according to the Mauna Loa Observatory in Hawaii [1]. The stepwise introduction of methanol up to 100 % by blending it with diesel leads to an increasing challenge due to its material compatibility. Methanol as a substance from the group of alcohols is commonly used as a cleaning agent that is among the top five of most widely traded chemicals in the world [2]. While the material behavior of the valve spindle/seat ring wear pairing is well known for the common fuels HFO, MDO, LPG or CNG, there are several open questions regarding the material compatibility in a methanol-fueled engine. Sarathy et al. [3] reviewed the alcohol combustion chemistry, including methanol, listing the most relevant kinetic mechanisms. The exposure of engine components to methanol atmosphere and especially its combustion by-products such as methanoic acid raises the question of tribological compatibility. Only a single carbon atom compared to diesel it cannot sufficiently form the carbonaceous particulate matter that is needed to build up a wear-protective tribofilm on both seating faces of valve spindle and seat ring. In addition, material degradation in methanol due to corrosion is another aspect but this is not the subject of this paper.

The first reports about the use of alcohols date back around 100 years. Interestingly, Boyd states that butyl alcohol did not knock in any of the engines of the 1920s [4]. It demonstrates that the potential of alcohols as fuels was evident very early on. Methanol is well-known for its molecular polarity concerning material compatibility. In addition to elastomers, methanol can also attack metals. Due to the fact that it is the most aggressive of all alcohols, changes of the engine hardware are discussed that are needed when engines run on mid to high level blend, or pure methanol. Many authors reviewed the material issue [5, 6, 7]. Xiang [8] considers measures to improve fuel lubrication, increase anti-corrosion and anti-rust properties and protect certain metals. Yuen et al. [7] documented that the polar nature of the methanol molecule causes dry corrosion, but this type of corrosion is aggravated by ionic impurities such as chlorides. Walker et al. [9] reported about a synergistic effect of contaminants. Chloride ion, acetic ion and ethyl acetate in hydrous alcohol – alcohols are hygroscopic – can drive a many times greater corrosion than a single contaminant. Mattson et al. [10] observed increased wear in methanol-fueled engines, especially at low operating temperatures. Combustion by-products, for example methanoic acid, are considered to promote higher wear. Aihara [11] reports about the wear of sliding surfaces in methanol engines. The technical issue of wear is raised when methanol is used. Therefore, Märkisches Werk is working to better understand the effects of methanol and its combustion by-products on material behavior to offer methanol-compatible valve spindle/seat ring pairings for reliable operation in large engines.

This paper deals primarily with the first methanol generation of valve spindle/seat ring wear pairings intake and exhaust for retrofit and new engine buildings from a tribological point of view. For this purpose, a typical pairing, for reference, for diesel engines of a valve spindle with Stellite™-12 hardfacing against a cast steel seat ring from a field test of a methanol engine was investigated. Considering these field findings, a series of tests were planned and carried out with typical valve and seat ring materials 1.4718 (X45CrSi9-3), 1.4882 (LV21-43), 2.4952 (Nimonic80A) and MW WR Superalloy at 100 °C and at elevated 400 °C in three atmospheres: methanol, methanoic acid and, for reference, in ambient air. As no appropriate test equipment was commercially available for the specific test requirements, one was designed, constructed and rigged up.

2 FIELD TEST

The field test involved a diesel engine that was retrofitted with a low-pressure port-fuel injection for a dual-fuel diesel and methanol operation. The retrofitted engine is an established medium-speed engine in maritime applications with power output of approx. 200 kW per cylinder. The standard diesel valve spindle and seat ring pairings for intake and exhaust were used. The engine ran on diesel for a short starting period, before it was switched into the dual-fuel mode. The test run was about 500 h in total, using a mixture of 90 % methanol and 10 % diesel. In this case, the energetic ratio was given, so 90 % of the energy came from the methanol. After the test, four sets of valve spindles and seat rings for exhaust and intake side were investigated. The investigation included a tactile profilometry of the seating face for all valve spindles. Three profiles with a spacing of 120° between them were measured per part. For the valves a calculation of the wear rate by integration was feasible by comparing the worn surface profiles to a profile from a new valve. For the seat rings this was not possible due to a lack of reference surfaces.

Additionally, one set of valve and seat ring were chosen for exhaust and intake side to carry out a more in-depth analysis by taking samples and analyzing the cross-sections via scanning electron microscopy (SEM) and energy-dispersive

spectroscopy (EDS). During the SEM analysis, particular attention was paid to the seating faces to investigate the wear mechanisms and to those areas that were in contact with methanol and its combustion by-products.

3 EXPERIMENTALS

3.1 Test set up

A setup for wear tests in corrosive media, usable for material screenings, was not available commercially and thus, it was designed for this project (see figure 1). The test rig has to be able to contain methanol and its possible combustion by-product methanoic acid and allow reproducible wear testing under a relevant load regime. A twin-column test bench actuated by an electro-magnetic pulse system with high dynamic performance was the base. The axial-torsion systems can deliver up to 10 kN force, 100 Nm torque and 100 Hz. The necessary assumptions and their implementations in the test rig shall be described in this subchapter.

The setup was designed to have two bodies in contact with each other, representing the valve and seat ring. Lehmann [12] reports about the two main valve wear mechanisms in large engines, impact wear and sliding wear, whereas the wear pairing valve/seat ring is more sensitive to impact wear. In a first approach it was chosen to model the sliding wear and its influence by the tested media. The specimen design and the test routine are described in the subsequent subchapters.

To minimize the danger of explosion due to auto-ignition of methanol at 440 °C, the highest test temperature was chosen to be 400 °C. The two test temperatures of 100 °C and 400 °C were reached with a heated mount that the plate sample was screwed onto, while the temperature was controlled using a thermal element that reached into the container. The two tested media were methanol and methanoic acid (15 % diluted in water), brought into the container with a tubing that dispensed a small amount droplet-wise every 9 s. To shield the tension and torsion sensor, the container was positioned on a cooling platform. The container functioned as a safety device as well, as it held excess media back and prevented the test rig from corrosion.

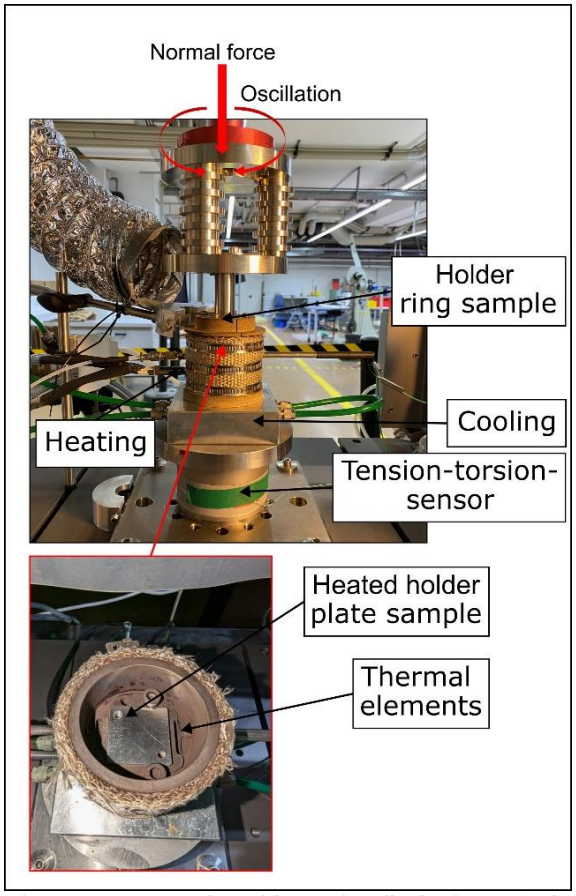

Figure 1: Test rig with a detailed view of the container.

3.2 Specimen

A ring-and-plate setup was chosen for the oscillating sliding wear test: a ring is pressed onto

Table 1: Nominal chemical composition and hardness of the tested materials.

Material \ Element	C (wt.-%)	Co (wt.-%)	Cr (wt.-%)	Fe (wt.-%)	Ni (wt.-%)	Mn (wt.-%)	Si (wt.-%)	W (wt.-%)	Others (wt.-%)	Hardness (HV30)
LV21-43 (X50CrMnNiNbN21-9)	0.45 – 0.55	-	20.0 – 22.0	Bal.	3.5 - 5.0	8.0 - 10.0	< 0.45	0.8 - 1.5	N=0.4-0.6; Nb=1.8-2.5	353 ± 6
Nimonic80A (NiCr20TiAl)	< 0.1	< 1.0	18.0 - 21.0	< 1.5	Bal.	< 1.0	< 1.0	-	Al=1.0-1.8; Ti=2.0-2.7	362 ± 6
X45CrSi9-3	0.40 - 0.50	-	8.50 - 10.00	Bal.	< 0.5	< 0.6	2.7 - 3.3	-	-	315 ± 6
Stellite™-12	1.60 - 1.80	Bal.	28.0 - 32.0	< 2.0	< 3.0	-	1.2 - 1.7	8.0 - 10.0	-	626 ± 20
MW WR Superalloy	Proprietary Co-base material									666 ± 10

a plate with a certain force and oscillates frequently to generate a relative motion of the surfaces.

The sample geometries in figures 2 and 3 were chosen so that the test bench would be able to apply a representative surface pressure between the contacting surfaces. An appropriate surface pressure value for all chosen materials had to be guaranteed while maintaining the manufacturability of the samples and the safe operation of the test rig. 90 MPa as typical geometrical surface pressure for the pairing valve spindle/seat ring in large diesel engines was chosen. For an initial ring surface of 22 mm², a force of 1980 N was necessary to yield 90 MPa of surface pressure.

In this setup, the ring was meant to represent the valve and thus was made of typical valve seating face materials: 1.4882 (LV21-43), 2.4952 (Nimonic80A), Stellite™-12 and MW WR Superalloy (Co-base hardfacing). The plates were made from 1.4718 (X45CrSi9-3) and from a MW WR Superalloy that MWH typically uses for seat rings. The nominal chemical composition of all tested materials are displayed in table 1. In the following, the materials shall be named according to the commercial name and not their chemical composition or alloy grade, except for X45CrSi9-3. The ring sample featured a wider lower part that was meant to be screwed to the upper holder of the test rig. The actual ring is situated on top of the wider part. The lower holder fastens the plate by a screw on the heating and inside the container.

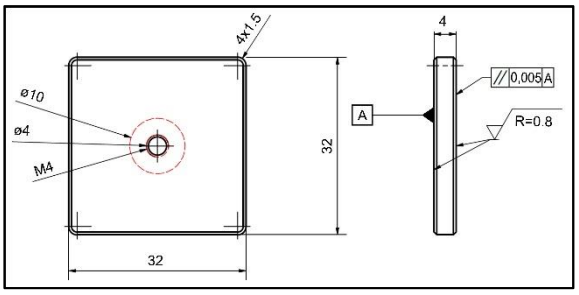

Figure 2: Geometry of the plate samples for the oscillating sliding wear tests.

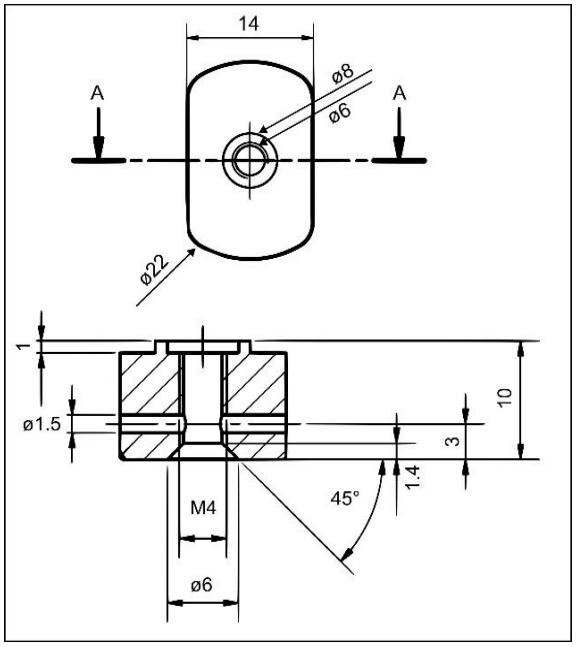

Figure 3: Geometry of the ring specimen for the oscillating sliding wear tests.

The rings made from LV21-43 and Nimonic80A were machined from stock material in a solution annealed condition with an application-relevant hardness of 353 HV30 and 362 HV30, respectively. The X45CrSi9-3 plates were extracted by eroding from surface milled slabs of stock material in a quenched and tempered condition with a hardness of 315 HV30.

Several layers of Stellite™-12 and MW WR Superalloy were PTA-welded on circular slabs of X45CrSi9-3, prepared with a half-circular shaped groove to allow a better weldability. From the PTA-welded discs, sample blanks were taken by eroding, after the welded material had been brought to a uniform height and surface finished by milling. The final ring geometry of the hardfaced samples was produced by milling, as well.

3.3 Test routine

Table 2: Test matrix with number of tests per parameter combination.

Material pairing		Atmosphere						Number of Tests
		Air		Methanol		Methanoic Acid		
Ring	Plate	100 °C	400 °C	100 °C	400 °C	200 °C	400 °C	
Stellite™-12	X45CrSi9-3	3	3	3	3	3	3	90
Nimonic80a	X45CrSi9-3	3	3	3	3	3	3	
LV21-43	X45CrSi9-3	3	3	3	3	3	3	
MW WR Superalloy	X45CrSi9-3	3	3	3	3	3	3	
MW WR Superalloy	MW WR Superalloy	3	3	3	3	3	3	

The test routine involved a repetitive oscillation of the ring sample for ± 3°, resulting in a sliding distance of ± 2 mm. The setup was heated up before each test for 10 min with closed contact between ring and plate to ensure an even temperature distribution. After the heating up time, the contact was separated for 1 min and then the procedure was started. The electrically powered test apparatus applied a constant force for a set of 9.000 oscillation cycles at the end of which the ring sample was lifted up. Eleven cycles summing up to approx. 100.000 cycles were carried out per test. The periodic lifting of the sample was included to interrupt the process and allow the interaction with the atmosphere. This should lead to a more realistic loading as the contact between valve and seat ring is not constantly closed in a real engine. Tribosystems that were already in a steady state of wear should be separated and then have to wear in again. This was meant to increase the influence of wear mechanisms and make the results easier to interpret. Three sliding wear tests were carried out per ring material combination against X45CrSi9-3 and additionally MW WR Superalloy was tested in self-contact (see the test plan in table 2). This test plan resulted in a total number of 90 tests carried out with 180 samples. During an initial test with methanoic acid at 100 °C, a highly corrosive slime was formed, which severely corroded the test chamber. In response, the lower test temperature for methanoic acid was raised to 200 °C to avoid damage to the test rig.

Every sample was macroscopically photographed before and after the test. Laser scanning microscope measurements of every samples was performed on a representative part of the worn surface. The wear rate was calculated by weighing the samples prior to and after the tests. For selected samples a SEM investigation was performed to get a deeper understanding of the underlying mechanisms.

4 RESULTS AND DISCUSSION

In this chapter the results from the field test and the test rig trials shall be displayed and reviewed separately. Especially the results from the test rig trials were numerous and thus a selection shall be displayed here to highlight the findings.

4.1 Field test

The calculated wear rates per hour are displayed in figure 4 for the intake and exhaust valves, averaged from four valves per side. The wear rate of the exhaust valves of 0.19 mm³/h is higher than that of the intake side with 0.12 mm³/h and, for reference, a state-of-the art exhaust valve spindle of about 0.10 mm³/h is illustrated as well. The small standard deviation of the two displayed averaged

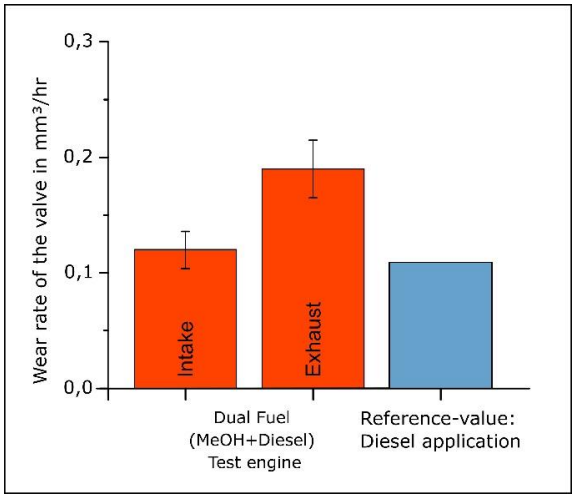

Figure 4: Wear rates of the intake and exhaust valves from the methanol dual fuel field test.

wear rates is an indication of a controlled and even wear development through the engine. Judging from the wear rates, the conclusion can be drawn that the conditions during the dual fuel engine operation were demanding on the components. The wear rates are still in the same order of magnitude as in the standard diesel application (0.1 mm³/h). On the intake side the wear rates are almost the same, but for the exhaust side a considerable increase is seen. Most concerns regarding the challenges of materials in methanol engines are related to corrosion or the superposition of corrosion and wear: tribocorrosion. Thus, a closer look at the actual parts had to be taken to assess the wear mechanisms.

Figure 5a-c show SEM pictures of cross-sectional cuts from an intake seat ring and valve. Figure 5a shows the X45CrSi9-3 valve seating face that was hardened up to 48 HRC on the outer diameter where the valve contacted the seat ring. The surface is smooth and displays only one chip, approx. 5 µm in size. The intake seat ring has a hardness of 44 HRC and is made from the cast steel GZ-X190CrMo12-2. Figure 5b shows a cross-section of the inner port surface of the seat ring where the mixture of methanol, diesel and air passes by. It can be seen that the steel matrix disconnects along the boundaries of the carbide network. It shall be noted that the investigated region of the seat ring is not in physical contact with the valve. There are no visible cracks that reach from the damaged area into the base material. Thus it is plausible that the disconnection of pieces of the steel matrix could be a corrosive attack along the phase boundaries of the carbide network, i.e. intercrystalline corrosion. Fig. 5c shows a cross-section of the intake seat ring as SEM picture. The middle of the seating face is heavily deformed about 15 µm deep. Dark material within the subsurface region indicates that a mechanical

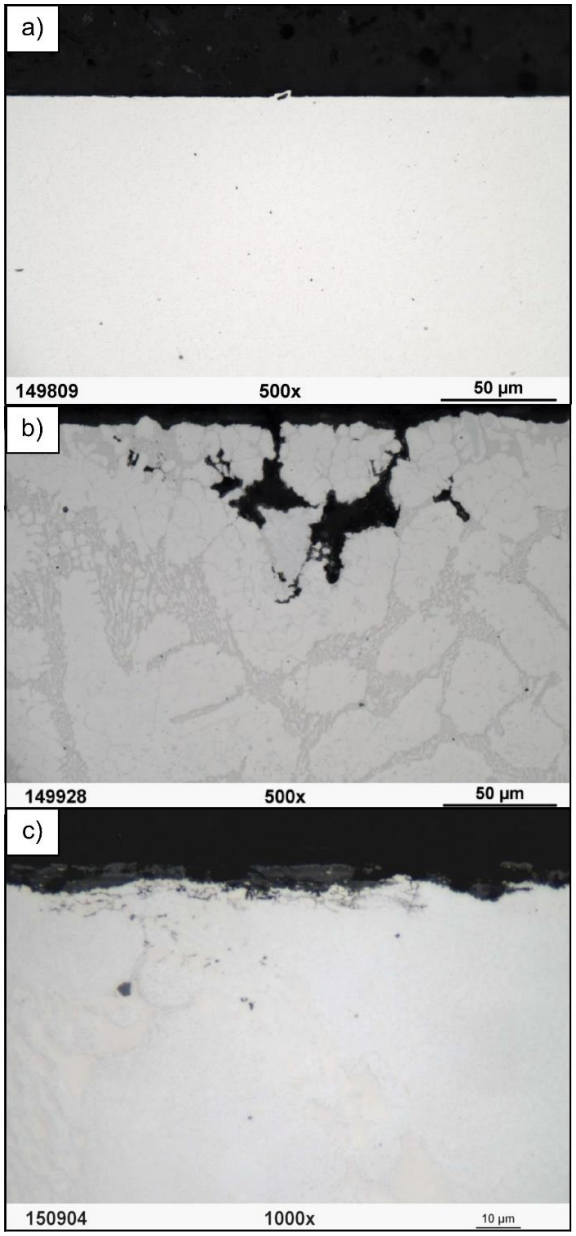

Figure 5: SEM-pictures from cross-sections of the intake side parts. a) valve seating face, outer diameter; b) seat ring, inner surface; c) seat ring, middle of seating face.

mixing of material took place. At this magnification no layer on the seating face can be seen and hence, the softer seat ring experienced heavy deformation due to the interaction with the hardened valve seating face. With the beginning of shearing to plastic deformation and followed by mechanical mixing in this zone, severe material damage can be seen, which led to outbreaks on the surface that are only few µm deep. Plastic deformation as the dominating wear mechanism can be concluded. Due to the plastic deformation of the subsurface zone, it cannot be judged whether the suspected intercrystalline corrosion took place on the seating face as well. The corrosive attack could have been driven by either a corrosive by-

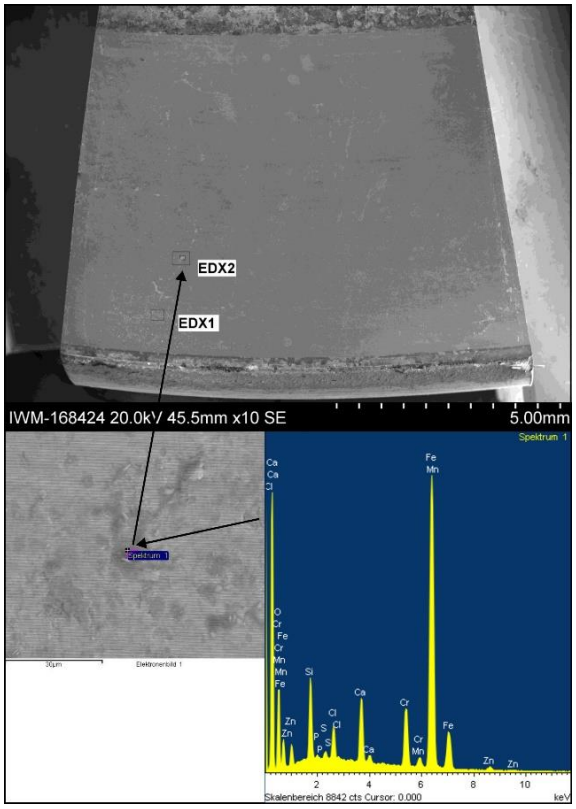

Figure 6: Intake valve seating face, detail of region “EDX2” and EDS-spectrum.

product of methanol like methanoic acid or another corrosive substance that was present. For instance, a common impurity of alcohols are chlorides and water which could serve as a corrosive media [13]. In a scenario where the engine is shut down and water vapor containing chlorides condensates on the cooled cylinder wall, this is plausible. EDS was used in this work to assess the chemical composition of residues on the seating faces. Besides typical combustion products (C, O) and oil additives (Ca, S, P, Zn), 2.5 wt.-% Cl were found on the seating face of the run intake valve spindle (see Figure 6). This is an indication of chloride induced corrosion to the wear phenomenon that is shown in figure 5b. Unfortunately, the engine run parameters do not allow for a tracing of influencing factors from the engine operation side. Still, the findings contradict the relatively small wear rate and put a question mark behind the long-term compatibility of standard diesel parts in dual fuel diesel/methanol-applications. On the exhaust side, the valve is hardfaced with Stellite™-12 which has a nominal hardness of 46 HRC. The exhaust seat ring is made of 44 HRC hard GZ-X190CrMo12-2 cast steel. Figure 7a-c shows cross-sectional SEM-pictures from the seating faces of the exhaust valve and seat ring. Figure 7a shows the subsurface zone of the valve seating face on the inner diameter in a region of contact between valve and seat ring.

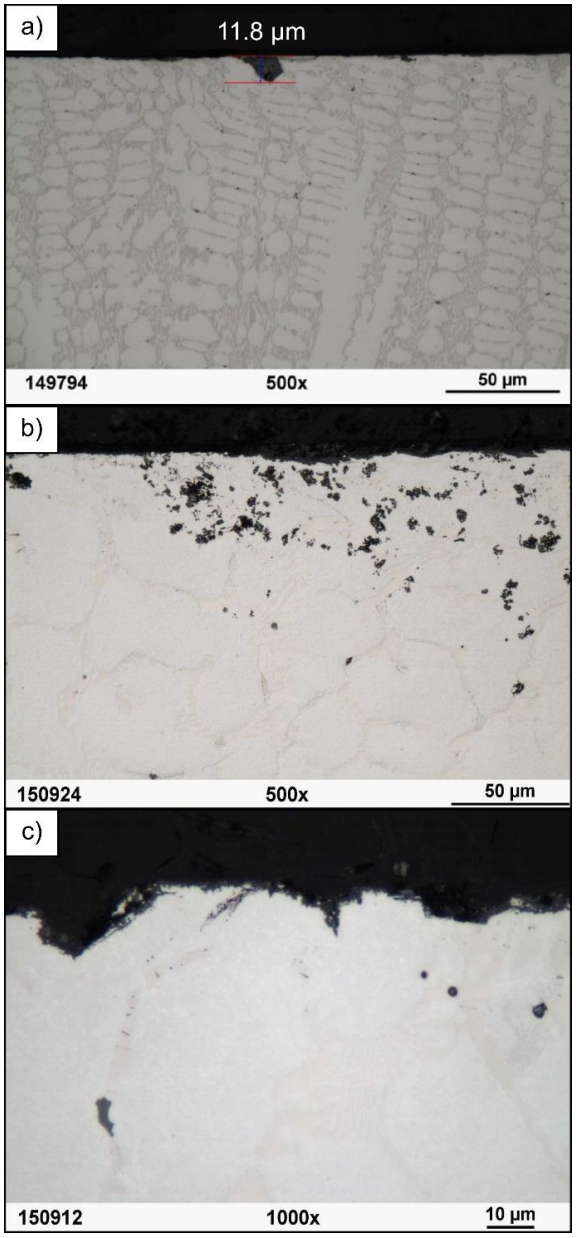

Figure 7: SEM-pictures from cross-sections of the exhaust side parts. a) valve seating face, inner diameter; b) seat ring middle of seating face c) seat ring seating face.

In the first 15 µm under the surface, a slight shearing is visible. The carbide network is sheared slightly to the left in the picture, but compared with the severe plastic deformation that Stellite™-12 can endure [14, 15], this has to be judged as only low deformation. Yet, an outbreak of a grain roughly 12 µm in size can be seen on the surface and such outbreaks were observed in other areas underneath the surface, as well. This behavior of the hardfacing differs from the frequently found wear mechanism that follows three steps [14, 15]:

1. Shear stresses are introduced to the subsurface zone primarily by the combustion pressure and secondly by valve closure.
2. Plastic deformation can be followed by mechanical mixing within the subsurface of the matrix, cracked and separated hard phases, surface oxides and combustion residues.
3. Delamination of heavily deformed particles: spalling.

The steps can repeat again and again and cause substantial wear rates, but in this case there is a limited plastic deformation within the subsurface zone.

The cross-sections of the seat ring in figures 7b-c display outbreaks and material mixing zones of the cast steel. The seat ring must have experienced a significant material activation of the first 50 µm underneath the surface. Broken hard phases, refined grains, surface foldings and embedded material within the first microns in the subsurface reach partially deep into the material. As mentioned above, a wear rate could not be determined for the seat rings, it seems plausible that the seat ring was worn more than the valve spindle. The outbreaks on the surface are approx. 15 µm deep and leave a rough surface. Broken out, deformed pieces of the seat ring and the valve might have been hard enough to cause additional damage as they were kept as a third body in the gap.

Summing up for the field tests, several concerning signs were found. The wear rate of the 500 hours run exhaust valve was significantly higher compared to a state-of-the-art valve. Yet, the material behavior found was noticeable. It is questionable if the wear rate would be stable for the next thousands of hours to come, which most applications would require, or if it would accelerate. The sharp-edged outbreaks found are not the typical wear phenomenon known for diesel and gas engines [15, 16]. Rather, the phenomena indicate a corrosive mechanism. Supported by the EDS findings, tribocorrosion seems to be the dominating wear mechanism. These findings are a clear indication for the need to conduct research projects to evaluate the compatibility of valve spindle and seat ring materials in methanol-fueled engines. The subsequent subchapter deals with the results from a research project that was initiated by MWH as a reaction to the presented field test findings.

4.2 Model test rig

In the course of this research, 90 trials were performed with the oscillating sliding wear test rig. The results shall be reviewed and discussed in this subchapter, bringing together the wear rates,

macroscopic and laser-optical pictures and selected SEM-images. The majority of results could be used to calculate averaged values of the wear rates per parameter set and per part. As three trials per parameter set were performed, it was possible to identify outliers and cross them out. At the end, 9 trials were identified as outliers and the results from 81 trials were considered for the averaged values and the discussion of results.

Figure 8 and figure 15 show the normalized values of wear rates in methanol and methanoic acid, respectively. The values are normalized to the highest wear rate that was measured in these tests: LV21-43 in methanoic acid at a temperature of 200 °C equal to 100 %. The diagrams are both created in the same way. The wear rates of the tested material, representing the valve, and the X45CrSi9-3 plate, representing the seat ring, are displayed as stacked bars. The bars stack up to a length that represents the wear of the entire system of tested material and steel plate. There is no overlap of the bars, as they are stacked to represent the wear rate for the system (valve spindle + seat ring). Only the topmost two bars are different, as they represent the self-pairing of the MW WR Superalloy. The slimmer bars represent the wear rates of the same parameters set in air for reference. A positive wear rate displays a loss of weight for the sample, while a negative rate means a gain of weight.

Test series in methanol:

The wear rate of LV21-43 and Nimonic80A at 100 °C are the highest of all oscillating wear tests, reaching to approx. 90 %. The wear of the valve material was slightly higher than that of the seat ring material in these tests. The rate was so high in fact that the LV21-43 tests were stopped at 40.000 - 60.000 cycles, as there was so much wear on the ring sample that the ground plate was in full contact. Compared to the reference wear rate in air, the wear was much higher in the methanol tests at 100 °C. At 400 °C, the wear rate for Nimonic80A and LV21-43 was reduced to approx. 12.5 %, with only slight wear on the valve material and most of the wear on the seat ring material. As all other parameters were kept the same, this can only be attributed to the increased temperature. Figure 9 displays results of an oscillating wear test with LV21-43 against X45CrSi9-3 at 100 °C that had to be stopped prematurely due to highest wear rate. The wear track on the X45CrSi9-3 plate is approx. 200 µm deep (figure 9c) and the LV21-43 ring is only 420 µm high, while it was 1 mm high at the beginning. Both worn samples show slight burrs that formed at the sides of the wear track. The macroscopic pictures show a dark discoloration of

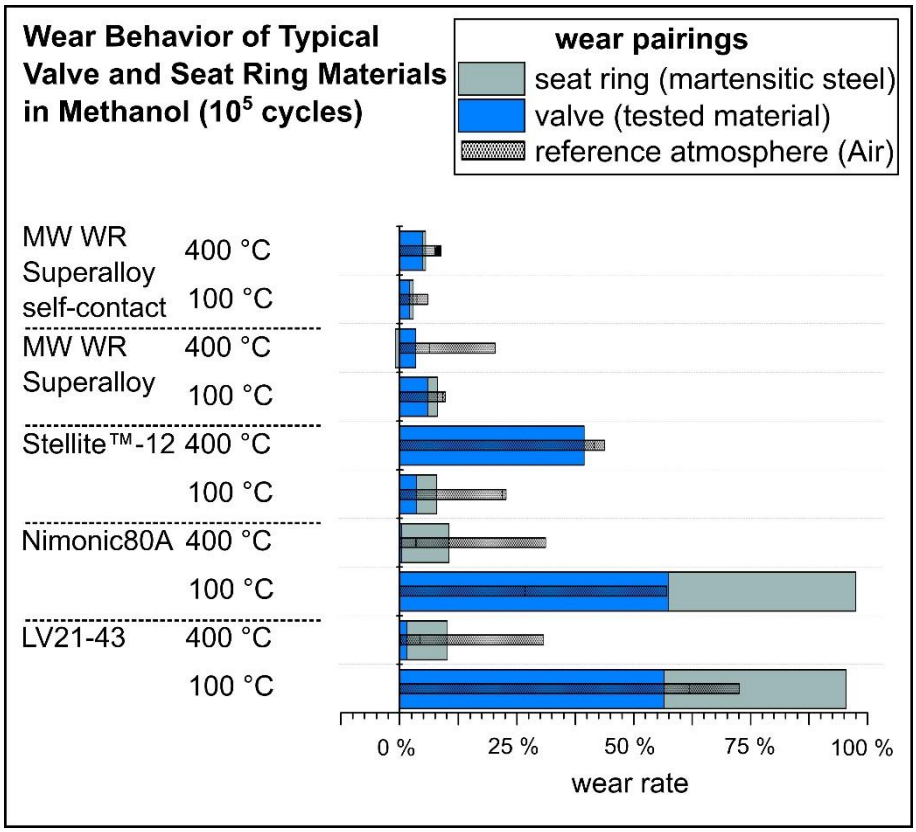

Figure 8: Normalized wear rates from test rig trials with different material combinations and at different temperatures in methanol.

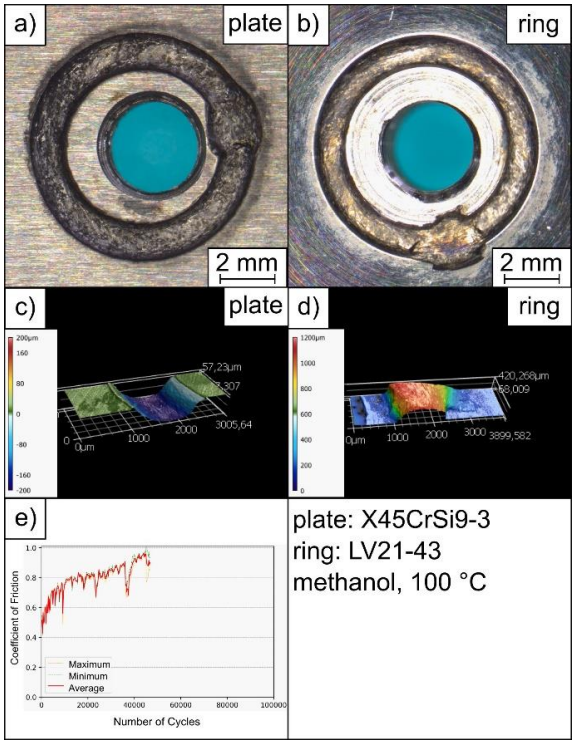

Figure 9: Ring: LV21-43, Plate: X45CrSi9-3, 100°C, tested in methanol. Macroscopic pictures of the plate and ring sample (a, b), 3D-laser scanning images with height information of plate an ring (c, d) and coefficient of friction plotted against number of cycles.

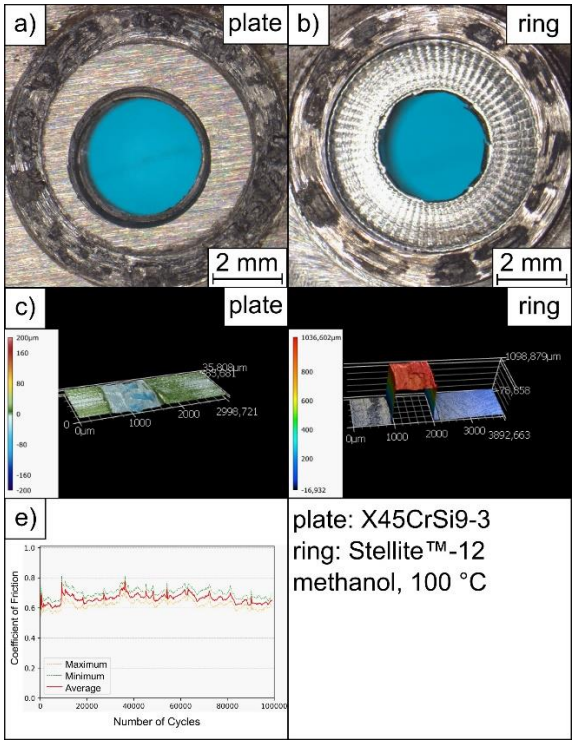

Figure 10: Ring: Stellite™-12, Plate: X45CrSi9-3, 100°C, tested in methanol. Macroscopic pictures of the plate and ring sample (a, b), 3D-laser scanning images with height information of plate an ring (c, d) and coefficient of friction plotted against number of cycles.

the plates wear track, while the ring is only dull in some points, but metallically shiny in most spots. The dark coloration of the plates wear track was found to be caused by corrosion and wear particles in the groove. No signs of adhesion were found on either of the bodies which is in accordance with the all positive wear rates. The coefficient of friction (COF) for this trial started at approx. 0.5 and kept increasing until the test had to be stopped at a COF of approx. 0.95 at approx. cycles 50.000. The COF plot shows an unsteady behavior that is not only due to the disengagement of the two bodies every 9.000 cycles. It is known from literature that during sliding wear austenitic steels like LV21-43 can show high wear rates due to a subsurface deformation, a formation of a tribological layer and its detachment [17]. The buildup of such layers and the subsequent detachment is a plausible explanation of the high wear rate, being purely abrasive, and the high COF. The described wear mechanism was found to occur for dry sliding wear in air. The wear in the methanol sliding wear tests was significantly higher. The surface of the plate wear track was found to be very rough in the laser scanning images (figure 9c). The roughness appeared to be higher than on the surface in other experiments and that could be a sign of corrosion or adhesion. But since the macroscopic images and the wear rates did not show hints of adhesion, the likelihood for a tribocorrosive attack is given. Such an attack would also contribute to an explanation for the high wear rate in the trials in methanol. It is also known from literature that the wear rate of austenitic steels in sliding wear can decrease due to the formation of oxidic scales on the surface [17]. As methanol is a strong cleaning agent that acts on the surface, it is plausible that this formation is hindered under the influence of methanol and at relatively low temperatures (100 °C). This could also be an explanation for the high wear rates at 100 °C in methanol for Nimonic80A and LV21-43. The reduced wear rate at 400 °C both in methanol and air could be attributed to a higher formation kinetic of the oxidic scales, lowering the wear rate. At 400 °C the dispensed methanol drops boiled off in a few seconds, moving over the surface on a gas layer, until the next drops were dispensed. Thus, the samples were not covered in methanol at all time and a reaction with the atmosphere and formation of oxides were possible. The presence of liquid methanol in the friction gap for several seconds before it boiled off might have added at least some level of lubrication to the system. Keeping in mind

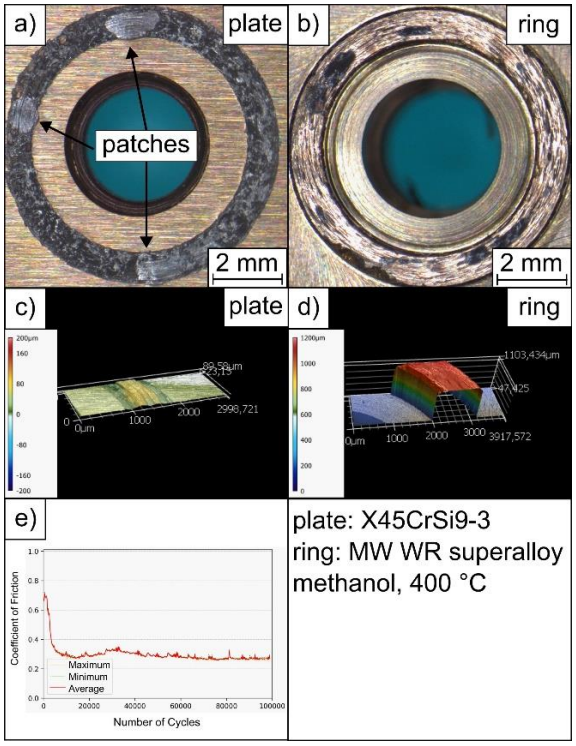

Figure 11: Ring: MW WR Superalloy, Plate: X45CrSi9-3, 400°C, tested in methanol. Macroscopic pictures of the plate and ring sample (a, b), 3D-laser scanning images with height information of plate and ring (c, d) and coefficient of friction plotted against number of cycles.

the earlier described wear mechanism, a small amount of lubrication can cause a reduction of subsurface deformation and thus hinder the delamination and the wear rate.

The wear rate of Stellite™-12 in methanol was lower than in air for both 100 °C and 400 °C. Contrary to Nimonic80A and LV21-43, the total wear increased with rising temperature. At 400 °C, the total wear rate of approx. 40 % was only measured on the valve material (ring sample), while at 100 °C the wear of approx. 10 % was equally distributed between ring and plate. Judging from the measured wear rates and the visual appearance of the samples, it was found that the wear was not purely abrasive as the positive wear rate would suggest. There are signs of adhesion, abrasion, surface disintegration and, at 100 °C, corrosion, as well. Adhesive wear of the both partners causes a transfer of material. It is true that the gravimetric measurement technique has a weakness in differentiating wear modes because if more material is lost from a body than is transferred, in total a weight loss can result even though adhesion is effective. It is thus important to have a close look at the worn surfaces to distinguish wear modes. In the case of

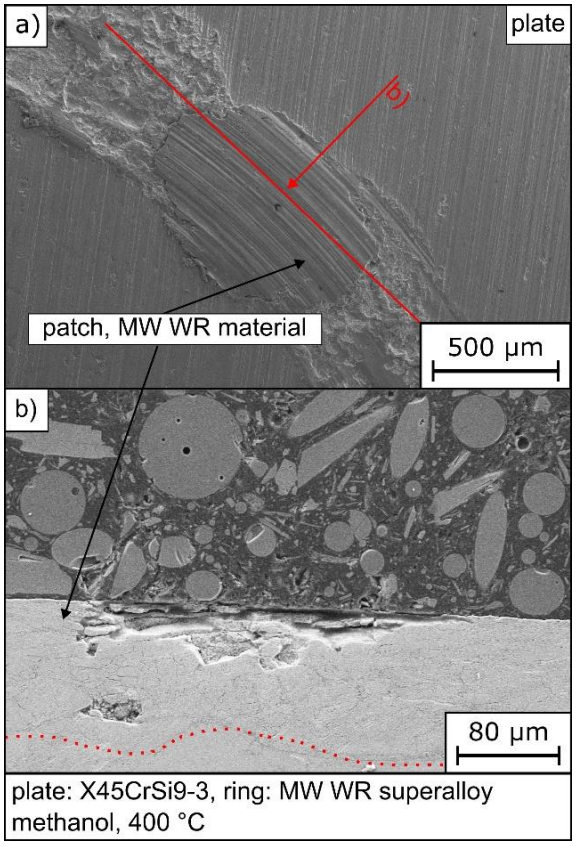

Figure 12: SEM-image of an X-45CrSi9-3 plate, tested against a MW WR Superalloy ring in methanol. a) showing the location and direction of the cross-section and b) showing the cross-section SEM-image.

Stellite™-12, the Co-base matrix material can be transferred and adhere to the wear track, but the hard phases are not deformable enough and break under shear loading. The fragments of hard phases are contributing to the abrasive wear and cause microgrooves on the surface that intersect. The repeatedly deformed surface material breaks out, causing a disintegration of the surface. The same traces of wear can be found at the Stellite™-12 samples from the 400°C trials in methanol (figure 10b,d). As discussed before, at 400 °C the methanol drops moved on a bed of steam for a short duration and then boiled off, resulting in less lubrication for the system at 400 °C. If the wear mechanisms are still present, the wear rate can be higher due to the higher adhesion tendency and lower strength of materials at higher temperatures. The findings are in line with Renz et al., who researched the performance of Stellite™-12 against a Cr-Mo steel in sliding wear tests at elevated temperatures [18, 19]. It was found that the hard phases of the Stellite™-12 acted as abrasives that caused massive wear, when they broke out. This behavior was mainly observed at 40 °C, while at higher temperatures the formation

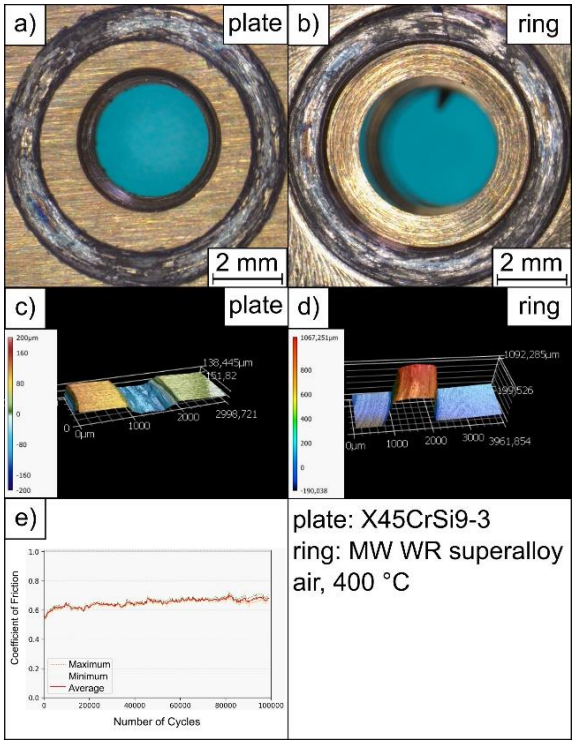

Figure 13: Ring: MW WR Superalloy, Plate: X45CrSi9-3, 400°C, tested in methanol. Macroscopic pictures of the plate and ring sample (a, b), 3D-laser scanning images with height information of plate and ring (c, d) and coefficient of friction plotted against number of cycles.

of oxides on the Cr-Mo steel counterbody protected it against wear quite effectively. In the oscillating sliding wear trials in methanol at 400 °C, the X45CrSi9-3 steel body was protected against the wear, as well, resulting in a wear rate that is not visible in the diagram. The Stellite™-12 showed increased wear in this work at 400 °C and it must be noted that the same behavior is also present in the reference results in air. It is plausible that the temperature of 400 °C is not sufficient for the Stellite™-12 to form and support a stable oxide layer, independent from the surrounding media in this particular test setup. Renz et al. discovered that a successful formation of oxides and protection of the Stellite™-12 was possible only at elevated temperatures of about 600 °C. It is also plausible that the formation of oxides were hindered in this case by the cleaning function of the methanol, which amplified the increase of wear rate with temperature. This behavior of the Stellite™-12 is in contrast to the findings on LV21-43 and Nimonic80A that were described earlier. Those two materials were able to reduce the wear successfully at higher temperature as they developed a stable oxide layer that could glide against the oxides on the X45CrSi9-3 steel surface.

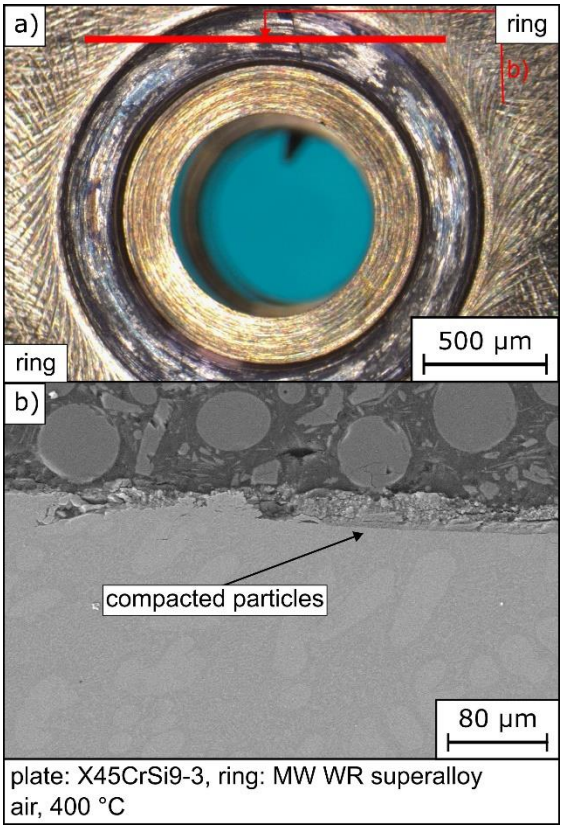

Figure 14: SEM-image of an X-45CrSi9-3 plate, tested against a MW WR Superalloy ring in methanol. a) showing the location and direction of the cross-section and b) showing the cross-section SEM-image.

The tribological performance of MW WR Superalloy in self-contact as well as in contact with the X45CrSi9-3 steel were overall the best at both tested temperatures 100°C and 400°C and both atmospheres air and methanol. The wear rates are in a range of below 10 % in all cases and the ring sample wears off more than the plate (X45CrSi9-3 and MW WR Superalloy). In the case of MW WR Superalloy vs. X45CrSi9-3 there is even a small weight gain of the sample. In figure 11, the explanation can be seen easily on the macroscopic image of the plate: patches of material are found in the wear track. The three patches are roughly elliptical and measure approx. 1.5 mm in length and 1 mm in width. Most of the contact during this test was between the surface of the MW WR Superalloy ring and the patches on the plate, made from the same material (see figure 11a). So in fact the tribosystem in this test was a self-contact of the MW WR Superalloy, as well. As a result of the contact between the patches and the ring surface, the COF was considerably low, indicating good tribological mating between the two surfaces. The wear of the MW WR Superalloy was even lower in methanol than in air. A cross-section image of the wear track on the MW WR Superalloy

ring after the 400 °C test in air against X45CrSi9-3 shows a wear-protective tribofilm of compacted wear particles on the surface (figure 14). This indicates that at 400 °C the formation of the patches and the resulting self-contact of very smooth Co-base surfaces, protects both surfaces well, while the oxide formation mechanisms cannot be effective. In contrast, the wear rate is lower in methanol than in air, which indicates a positive effect of the methanol on the wear behavior. This could be attributed to the cleaning effect of the surface that might help the build-up of the transferred material sections.

The MW WR Superalloy self-contact pairings in methanol showed the lowest wear rates of all tests. The beneficial conditions of self-contact that evolved in the MW WR Superalloy vs. X45CrSi9-3 tests was evident from the beginning in the self-contact tests. The wear tracks show layers of adhesively transferred material and compacted particles at the surfaces. There are no signs for the formation of a stable oxidic layer that might have reduced the wear. It seems to be the case that the self-contact with a tribofilm of transferred material is working well to reduce the wear, as it was in the previously described tests against the X45CrSi9-3 steel. At higher temperature a slight oxidation of the wear particles could have occurred which might be the cause for the slightly higher wear rate due to the higher hardness of the oxides. The wear behavior of the MW WR Superalloy shows the lowest wear rates compared to all other materials in methanol.

Test series in methanoic acid:

In self-contact and in contact with the X45CrSi9-3 steel plate, the MW WR Superalloy was the best performing tested valve material in methanol. LV21-43 tests had to be canceled prematurely due to the highest wear rate. Similar trends can be seen in the methanoic acid tests – wear rates are displayed in figure 15. The wear rates were normalized to the same scale like those from the methanol tests (figure 8).

LV21-43 and Nimonic80A have high wear rates at 200 °C in the methanoic acid tests and the rate decreases with rising temperature. At 200 °C the wear is nearly evenly distributed between LV21-43 and the X45CrSi9-3 steel. At 400 °C, the plate wears more than the ring. The wear rate of the Nimonic80A ring was small in comparison to the X45CrSi9-3 steel plate (approx. 45% to approx. 5%), and with rising temperature the ring showed nearly no wear. In principle, this is the same behavior that was described earlier for the same materials in the methanol tests. Just like for the tests in methanol, the worn surfaces of LV21-43

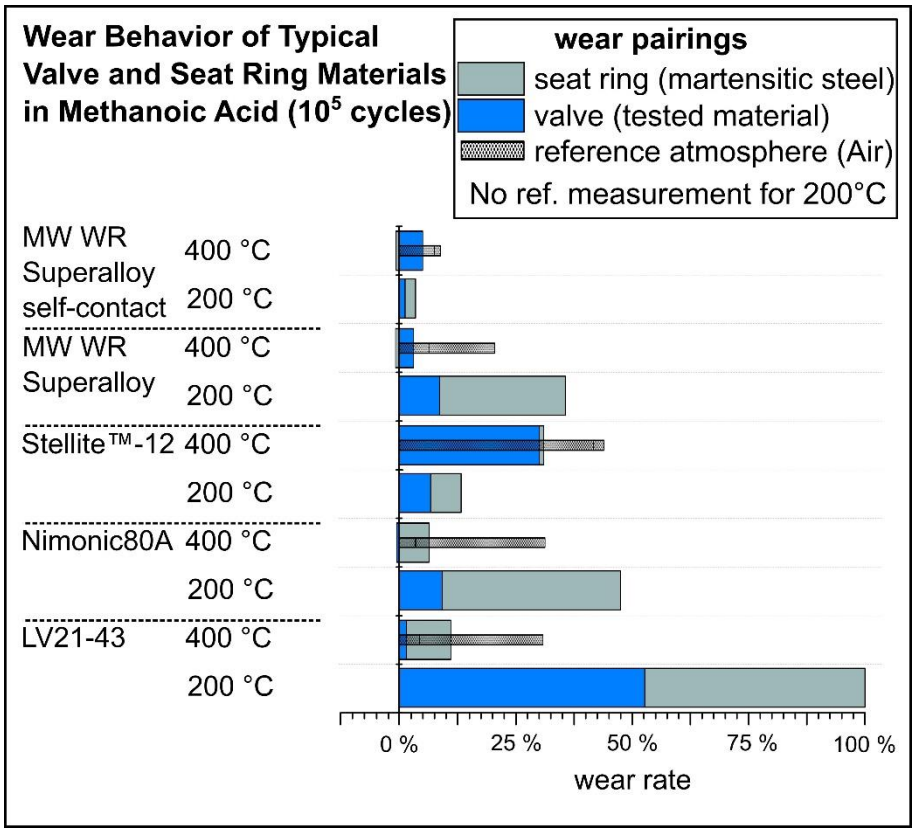

Figure 15: Normalized wear rates from test rig trials with different material combinations and at different temperatures in methanoic acid.

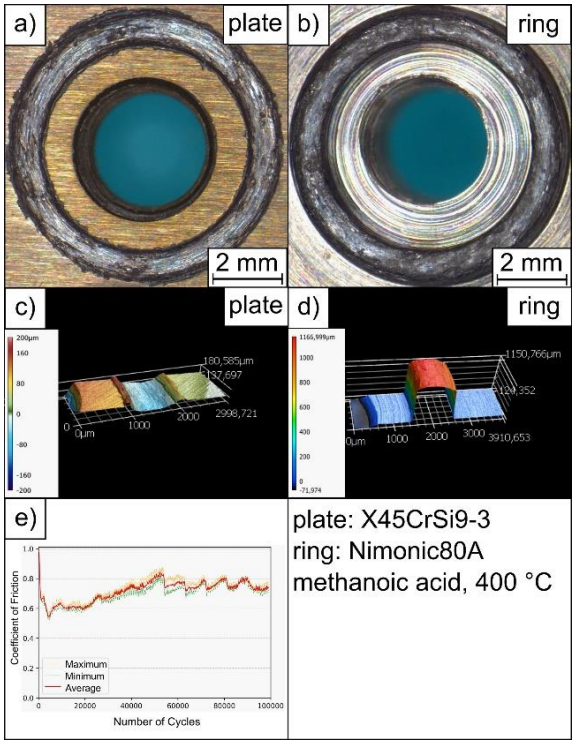

Figure 16: Ring: Nimonic80A, Plate: X45CrSi9-3, 400°C, tested in methanoic acid. Macroscopic pictures of the plate and ring sample (a, b), 3D-laser scanning images with height information of plate and ring (c, d) and coefficient of friction plotted against number of cycles.

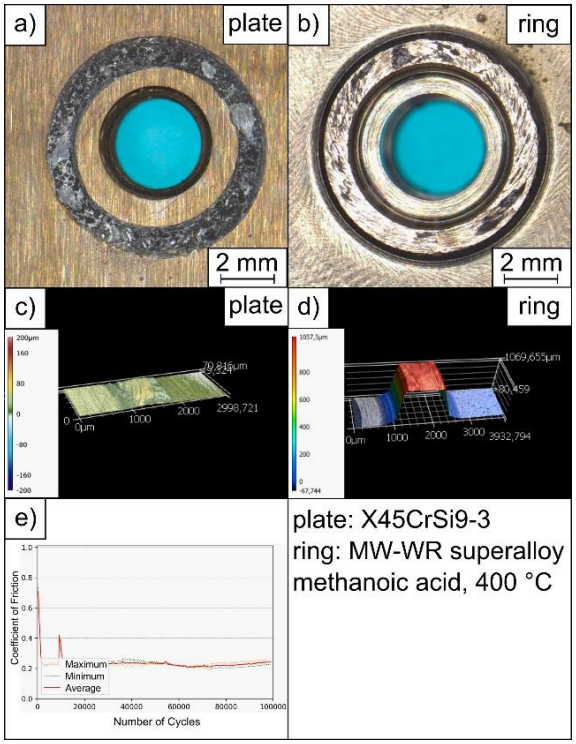

Figure 17: Ring: MW WR Superalloy, Plate: X45CrSi9-3, 400°C, tested in methanoic acid. Macroscopic pictures of the plate and ring sample (a, b), 3D-laser scanning images with height information of plate and ring (c, d) and coefficient of friction plotted against number of cycles.

and Nimonic80A showed no signs of adhesion, but compacted wear particles, grooves and slight corrosion marks (see figure 16). It appears that the lack of formation of wear-protective oxide layers is still a problem at 200 °C for both materials, even though the wear of Nimonic80A is lower in methanoic acid than in methanol. No additional effect, accounting for the behavior in methanol can be seen for LV21-43 and Nimonic80A.

The wear rates and macroscopic pictures of the tests with Stellite™-12 in methanoic acid did not show any new features compared to those from methanol tests, as well. The wear rates at the tested temperatures and the observations made on the surfaces were very much comparable. As no differing behavior and as the Stellite™-12 wear rates were not the outstanding in either a good or bad way, pictures are not shown for the sake of conciseness.

Figure 17 shows the results of the test with MW WR Superalloy against the X45CrSi9-3 steel plate at 400 °C in methanoic acid. The COF was approx. 0.2 which is one of the lowest measured values. On the plate-sample patches of ring material were formed which is the same behavior as in the methanol tests with the same parameters.

With the exception of the 200 °C wear rate being quite high (approx. 42 %) for the same combination, MW WR Superalloy performed as well as in the tests in methanol. The tests at 200 °C with the high wear rate featured a high seat ring wear. There were no patches of material found on the plates after these tests which indicates that 200 °C is still not high enough for them to form. The harder MW WR Superalloy (see table 1) can then easily wear the softer, annealed martensitic X45CrSi9-3 steel. At 200 °C the methanoic acid – water solution was boiling off quickly, preventing liquid residue to serve as a lubrication. In this way, high wear rates of the plate are possibly explainable. The wear behavior of the MW WR Superalloy shows the lowest wear rates compared to all other materials in methanoic acid.

5 SUMMARY AND CONCLUSION

This paper presents results from a field test and test series of a bespoke model test rig, aiming to develop the first generation of methanol valve spindle and seat ring pairings for intake and exhaust. For this purpose the effects of methanol and its combustion by-product methanoic acid on the wear behavior of typical valve and seat ring materials were investigated. The field test was

performed with standard diesel components in a retrofitted diesel engine with a low-pressure methanol port-fuel injection. Wear rate computation, except seat rings and detailed electron-optical analysis were performed on the valves and seat rings of the intake and exhaust site. The test rig was specially designed to quantify the wear behavior of typical valve and seat ring materials in methanol and methanoic acid at two temperatures 100°C and 400 °C. Laser-optical analysis and gravimetric wear rate computation was performed on each of the 180 samples from the 90 experiments. Additional investigations were carried out on selected samples.

The key findings can be summarized as follows:

Field test:

- The standard diesel parts showed an increased wear rate regarding the exhaust valve spindle of about 0.19 mm³/h compared to a state-of-the-art wear rate of 0.10 mm³/h and the observed wear phenomena are not typical for diesel and gas engines. Both the Stellite™-12 valve hardfacing and the cast steel seat ring showed a sharp-edged, partially fissured surface topography extended by outbreaks. In contrast to diesel and gas engines, tribocorrosion as main wear mechanism can be assumed in methanol engines.

Model test rig trials:

- The austenitic steel LV21-43 and the Ni-base material Nimonic80A showed the highest wear rates at 100 °C in both atmospheres methanol and methanoic acid. The wear was mainly abrasive. At 100 °C and 200 °C a wear-protective layer could not form and the wear was even higher than in air which is a hint for a methanol-enhanced wear. At 400 °C the wear was quite low in both tested media, which indicates that a wear-protective tribofilm was formed successfully.

- Stellite™-12 was the only material that showed a substantial increase in wear rate with increasing temperature. This was related to the apparent lack of formation of wear-protective layers even at higher temperatures (400 °C), which may have been too low according to literature. As a result, the breaking out of hard wear particles from the adhering, transferred Stellite™-12 material was not hindered and could even cause more damage at higher temperatures.

- Overall, MW WR Superalloy showed the lowest wear rates in the model test rig trials in methanol as well as in methanoic acid. At 400 °C this was attributed to the formation of patches from MW WR Superalloy material that was transferred to the opposing body. At lower temperatures, the MW WR Superalloy showed the excellent performance that it is known to deliver in dry sliding wear. The performance in self-contact shows the lowest wear rate of all material pairings.

The following conclusions can be drawn from the findings:

- In light of the long-term operation of a valve spindle or a seat ring, it is questionable if the increased wear rate in the field test would suddenly decrease or instead accelerate over time due to the observed wear mechanisms. At least it can be concluded from the first 500 operation hours that the material choice should be reviewed and the longevity of the parts remains questionable.

- Judging from the experiments, a combination of valve and seat ring both hardfaced with MW WR Superalloy is the best choice for usage in methanol applications at both high and low temperatures. Based on the results from the model test rig trials and the field test, Märkisches Werk GmbH presents the first generation of methanol valve spindles and seat rings for intake and exhaust.

- It was found that methanoic acid had no additional negative or positive effect on the wear rate of the tested material compared to methanol. The observed mechanisms and the basic trend regarding temperatures and material pairing are valid for both.

- When it comes to the base material, no statement can be derived. In this project work, only the tribological point of view regarding sliding wear was tested. It can be stated that in the field test as well as in the model test rig trials, signs for corrosive attack have been seen. This motivates further project work – corrosion tests are necessary to develop further answers in the field of material compatibility.

6 OUTLOOK

Alcohols are aggressive towards magnesium, aluminum and copper. It is known that steel and other ferrous metals are slightly affected. To clarify the corrosion behavior of typical valve materials in methanol and methanoic acid, Märkisches Werk has initiated a further research project.

7 REFERENCES AND BIBLIOGRAPHY

[1] https://gml.noaa.gov/ccgg/trends/.

[2] ICIS, Chemical profile special, ICIS Chemical Business (26 May – 1 June 2017).

[3] Sarathy, S. M., Osswald, P., Hansen, N. et al., 2014, Alcohol combustion chemistry, Progress in Energy and Combustion Science 44, 40-102.

[4] Boyd, T., 1950, Pathfinding in fuels and engines, SAE Q Trans 4, 182–195.

[5] Hagen, D.L., Methanol as a fuel: a review with bibliography, 1977, SAE paper no. 770792.

[6] McCoy, G. A., Kerstetter, J., Lyons, J. K., 1993, Alcohol-fueled vehicles, Tech. Rep. WSE-93/25, Washington State Energy Office.

[7] Yuen, P. K. P., Villaire, W., Beckett, J., 2010, Automotive materials engineering challenges and solutions for the use of ethanol and methanol blended fuels, 2010, SAE paper no. 2010-01-0729.

[8] Xiang, X., 2015, Introduction of Jetsun methanol fuel additives and engine oils, Tech. rep., Guangzhou Jetsun Lubrication Technology Co., Ltd..

[9] Walker, M., Chance, R., 1983, Corrosion of metals and the effectiveness of inhibitors in ethanol fuels, SAE paper no. 831828.

[10] Mattson, L., Olsson, B., Nilsson, P. H., Wirmark, G.,1993, Wear and film formation in the presence of methanol and formic acid, Wear, Volume 165, Issue 1, 75-83.

[11] Aihara, H., 1994, Tribology for alternative-fuel engines, Tribology International Volume 27, Issue 1, 51-56.

[12] Lehmann, O., 2018, Neuartiger Ansatz zur Untersuchung des tribologischen Systems Ventilspindel/Sitzring für Großgasmotoren, Fortschritt-Berichte VDI, Reihe 12, ISBN 978-3-18-381212-7.

[13] Käfer, S., Melz, T., Engler, T., Oechsner, M., 2019, Einfluss biogener Kraftstoffe auf das Ermüdungsverhalten von Stählen, Motortechnische Zeitschrift (MTZ), Issue 11/2019, 106-111.

[14] Lehmann, O., Renz, A., 2016, Valve wear in lean-burn large bore gas engines – From engine tests of components to a unique tribological test rig, CIMAC World Congress, Paper No. 231, Helsinki, Finland.

[15] Lehmann, O., Scherge, M., Renz, A., 2015, Wear mechanism study of Stellite-hardfaced combustion inlet valve spindles in lean-burn large bore gas engines, Dessauer Gas Engine Conference, conference proceeding, 137-145.

[16] Forsberg, P., Hollmann, P. Jacobson, S., 2011, Wear mechanism study of exhaust valve system in modern heavy duty combustion engines, Wear, Volume 271, 2477-2484.

[17] Straffelini, G., Molinari, A., Trabucco, D., 2002, Sliding wear of austenitic and austenitic-ferritic stainless steels, Metall Mater Trans A 33, 613–624.

[18] Renz, A., Prakash, B., Hardell, J., Lehmann, O., 2018, High-temperature sliding wear behaviour of Stellite® 12 and Tribaloy® T400, Wear, Volumes 402-403, 148-159.

[19] Renz, A., Kürten, D., Lehmann, O., Wear of hardfaced valve spindles in highly loaded stationary lean-burn large bore gas engines, Wear, Volumes 376-377, 1652-1661.